ISSN 2354-9114 (online), ISSN 0024-9521 (print)
Indonesian Journal of Geography Vol.53 , No. 2, 2021 (192 – 197)
DOI: http://dx.doi.org/10.22146/ijg.54247 website: https://jurnal.ugm.ac.id/ijg
©2021 Faculty of Geography UGM and The Indonesian Geographers Association

INDONESIAN JOURNAL OF GEOGRAPHY

RESEARCH ARTICLE

Preliminary Determination of Footprint Area of Uncontrolled Space Debris: Case Study of Tiangong-1 Space Station

Ahmad N[1] and Fitri E[2]
[1]Indonesian National Institute of Aeronautics and Space – LAPAN
[2]Astronomi Department, Insitut Teknologi Bandung - ITB

Received: 2020-04-11
Accepted: 2021-06-24

Keywords:
Footprint area;
Tiangong-1;
Space debris

Correspondent email:
nizam.ahmad@lapan.go.id

Abstract. Indonesia is an archipelagic country consisting of 16,056 islands and covering a vast area around 5,120km x 1,760km. With the largest coastline in the world, Indonesia is vulnerable to the fall of human-made objects from space. Furthermore, the space objects placed at polar and equatorial regions pass over the equatorial region, including Indonesia, more frequently around 4 and 9 times a day, successively depending on their altitudes. Due to the significant probability of the passages, determining the footprint of falling space objects (debris) is mandatory. Therefore, this study examines the demise of Tiangong 1 as a case study. First, trajectory propagation was carried out to track the re-entry point resulting in an estimated footprint area of around 2,632 km x 2,698 km over the Sothern Pacific Ocean. Second, a mathematical formulation in Astrodynamics was applied to engage a series of assumptions, which led to a more cramped footprint area of around 193km x 12km over a small portion of the South Pacific Ocean. Since the orbital prediction is fraught with great uncertainty, it was very likely that the Tiangong-1 debris fell over the Southern Pacific Ocean of the order of thousands of kilometers.

©2021 by the authors. Licensee Indonesian Journal of Geography, Indonesia.
This article is an open access article distributed under the terms and conditions of the Creative Commons Attribution(CC BY NC) licensehttps://creativecommons.org/licenses/by-nc/4.0/.

Nomenclature

Apogee height : the furthest distance between satellite and Earth
Argument of perigee (w): The orientation of an object in the orbital plane in the direction of satellite's motion.
Atmospheric drag : Perturbation force in space that can reduce the satellite altitude
Decay rate : the rate of degradation of satellite mean motion per day
Decay/re-entry window : The decay rate as well as proximate re-entry time of decaying object.
Eccentricity (e) : The shape of an orbit in the form of circle, ellipse, parabola and hyperbola
Ground footprint : Estimated area of falling space debris impact on Earth
Inclination (i): tilt of the orbital plane of spacecraft from the Earth equatorial plane (unit: degree (deg))
Mean anomaly (M) : The fraction of period of an orbit in the course of one orbital revolution
Mean motion (n) : The angular speed of satellite in one orbital revolution
Perigee height : the closest distance between satellite and Earth
Right ascencion of the ascending node (W) : The orientation of an object in the orbital plane measured from the vernal equinox to the ascending node
Simplified General Perturbations (SGP): Orbital propagator that counts the atmospheric drag as well as Earth oblateness and gravitational effects of the sun and moon.
Space debris / space junk : Inactive artificial objects in space from varoius sources such as inactive spacecraft, deserted payloads and launch vechicles, fragmentation, etc.

1. Introduction

The growth of space population made by humans over the course of the years not only affects the safety of satellite launches into space but also gives rise to distress to the human population on Earth. Human activities depend on the space-based infrastructure, therefore the rise is unavoidable, i.e., communication, navigation, remote sensing, etc. Moreover, finding a solution to reduce these inactive satellites or space debris is difficult because it is complicated, and the removal or disposal process requires expensive technology. The increase in space population is caused by several factors, including the growth of users over the year, which has led to an increasing number of launched satellites. (SIA, 2017) The need to neutralize idle satellites by Anti-Satellite weapon (ASAT) technology generates thousands of new fragments (e.g. Fengyun 1C DEB in 2007), which aggravated the issue of space debris (NASA, 2014) the collision between space junks and an active satellite (e.g. Fengyun 1C DEB vs BLITS in 2013). (Kelso et al., 2013) The hypervelocity impingement of two active satellites (e.g. Iridium 33 vs Cosmos 2251 in 2009). (Tan et al., 2013) The creation of at least a million pieces of debris of various sizes.

Obviously, an active satellite with space debris has a long shelf life, however, it is removed or naturally disposed of its initial orbit in the presence of perturbation. For example, gravitation from other celestial bodies such as asteroid and

comet or total loss caused by high-energy particles from the sun through charging effects. Furthermore, the space objects placed at more than 600km altitude outlast for 100 years encircling the Earth much longer than its operational lifetime. To combat the potential collision among non-operational objects like space debris, such an assessment is important for mitigation.

In the past few years, a progressive observation done by Space Surveillance Network (SSN) has tracked and cataloged more than 20,000 objects (Stansbery, 2004). Based on the statistical model, there are ~34,000 objects with a size of more than 10cm orbiting the Earth with a speed of ~7.8km/s. Considering the impact risk analysis, especially for falling space debris, such an effort to determine a footprint area needs to be made.

Indonesia is vulnerable to the fall of debris space because it is the largest archipelagic country in the world (16,056 islands in 2019; https://www.bps.go.id/), stretching around 5,120km along the equator and 1,760km from north to south. Furthermore, the country has the 2nd largest coastline in the world. A rough estimate has been made that polar and equatorial near-Earth orbiting objects pass through the region around 4 and 9 times daily, depending on their altitude. Both polar and equatorial space objects have a great probability of surpassing Indonesian territory, therefore, it is important to determine the footprint. In this study, a preliminary determination of the footprint area of falling space debris was carried out by solely taking into account the unperturbed orbit of a space object as a case study.

2. Methods

Orbital data in the form of Two Line Element (TLE) set data (www.space-track.org) consisting of some information, i.e. inclination (i), right ascension of the ascending node (Ω), the argument of perigee (ω), mean anomaly (M), eccentricity (e) and mean motion (n) were adopted. The first four parameters represent the orientation of the orbital plane, while the rest delineate its as well as the average angular rate of motion per orbit, respectively (Vallado, 2001).

The Tiangong-1 space station was also adopted, and this object discontinued regular orbital maneuvers since 2016 and fell to Earth in April 2018 (Vellutini et al., 2020). Tiangong-1 is China's first space station module placed at ~370km altitude and 43° inclination. Furthermore, communication with the station was lost and went out of control around March and September 2016, respectively. However, this object continuously degraded its altitude and was declared to have an orbital decay state in December 2016.

Since Tiangong-1 was not equipped with propulsion systems for orbital maneuver, the ground controller barely oversaw its re-entry point. Therefore, it was hard to precisely predict it as a single point rather than an area of impact called footprint. Accordingly, an attempt was made in this study to determine the footprint of Tiangong-1 by excluding variations of the Earth's rotation rate and tropospheric wind factor for simplicity. The steps of determination are described through the schematic diagram shown in Figure 1.

First, the altitude of the space object was diagnosed by looking for the evolution of its orbital height since its launch. It is evident that most low Earth orbiting (LEO) satellites undergo atmospheric drag leading to altitude loss. The rocket engines of onboard space objects were used to overcome this degradation. However, the majority of LEO spacecraft are

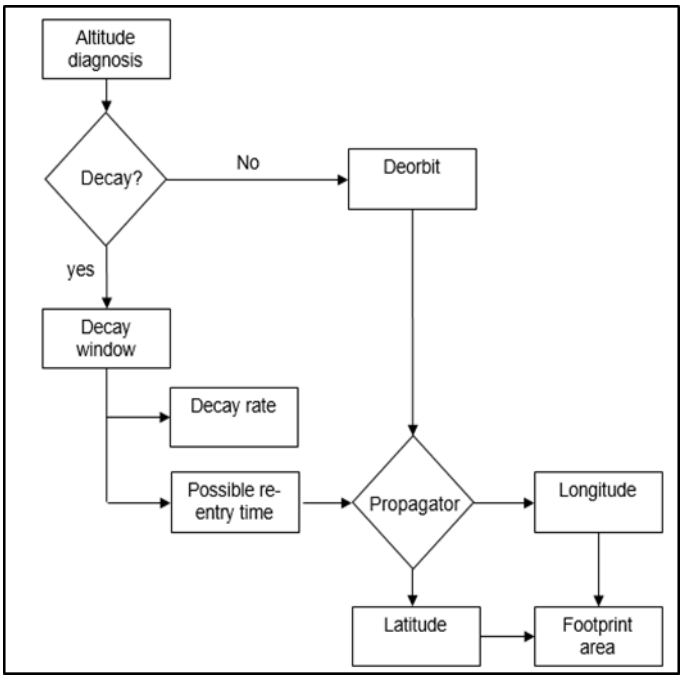

Figure 1. The Schematic diagram of footprint determination of falling space debris.

not equipped with rocket engines for orbital maneuver, therefore, a gradual decrease in their altitude is inevitable. This continuous decrease in orbital height led to the potential decay of space objects. In this state, it is easy to estimate the decay window consisting of a decay rate as well as a reasonable re-entry time. However, an issue arises in which TLE data and the imminent re-entry time is hardly accessible for some cases. To fix this, the Simplified General Perturbation 4 (SGP4) method was adopted for orbital propagation (Vallado et al., 2006). It should be noted that the SGP4 method has been adopted in the satellite tracking software called Orbitron (http://www.stoff.pl/), in which the step was practically conducted by employing orbitron. Besides the decaying orbit, atmospheric re-entry also occurs through deorbiting aging spacecraft. Therefore, both channels of occurrence need to be propagated to lessen uncertainty in estimating the re-entry point. Propagating the spacecraft position close to the re-entry time is expected to give a predictive geographical location object (latitude and longitude), which indirectly implied a footprint of surviving debris.

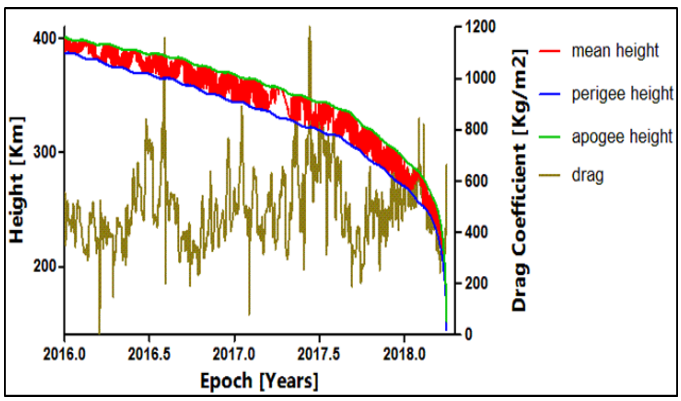

Figure 2. Evolution of Tiangong-1 altitude from 2016 to 2018. The mean, perigee and apogee altitudes are indicated by the red, blue and green lines, respectively, whereas drag effect is indicated by the gold line.

3. Results and Discussion

The evolution of Tiangong-1 altitude was first shown from the altitude loss in December 2016 until the re-entry window on March 29 to April 2018 (http://www.satflare.com/). The height evolution is shown in Figure 2.

Figure 2 describes a gradual decrease of Tiangong-1 altitude spanning from early December 2016 to re-entry imminent. Since TLE data is generated by using an orbital propagator SGP4, the effect of atmospheric drag, in the form of drag coefficient, on satellite altitude is included. Therefore, a specific atmospheric model which affected the accuracy of the calculation was neglected in this study. Furthermore, the prediction made using a satellite orbital decay calculator, namely SatEvo, developed by Alan Pickup, results in dissented re-entry time. In this case, Tiangong-1 will re-enter the atmosphere after 413.8534 days or around January 19 2018. Notice that the initial altitude is taken (350 km), and the starting point of calculation is determined when Tiangong 1 is detected to have an orbital reduction in late 2016. The spacecraft mass is around 8506kg and cross-section area of 129.18m^2 (Csillik, 2017). This prediction was undertaken during the period of low solar activity (solar minimum). Tiangong 1 re-entered Earth's atmosphere on April 2 2019 at 0:16 UTC (http://spaceflight101.com/). Regardless of erroneous prediction, the determination of footprint area is settled by considering the satellite position derived from the latest TLE set provided by Space-Track. The geographical position of Tiangong-1 in regard to the procurable TLE set is shown in Figure 3.

In Figure 3, the spacecraft's altitude is around 144km, which is higher than the average re-entry of 120km. It is important to note that there is no strict border of re-entry altitude. This appraisal is made in terms of the effects of atmospheric drag on satellite orbit, which gradually slows the orbital speed of spacecraft and it commonly occurs at ~120km altitude (Stamminger, 2007). Therefore, to procure the re-entry point below ~120 km altitude, in the absence of Space-Track data, orbital propagation need to be undertaken. Assuming that the orbitron propagated the Tiangong-1 trajectory up to April 2, 2018, at 0:16 UTC, the location of this object can be seen in Figure 5.

Furthermore, an attempt was made to calculate the decay rate of Tiangong-1 referring to its orbital revolution and the result showed a high rate of ~ 0.02 rev/day^2 (Figure 4), in addition to the average height loss of 10km. Note that the decay rate is taken by pondering the change of daily mean motion, which is incorporated in TLE data (Kennewel, 1999). Furthermore, the drag coefficient is one of the parameters that contribute to the determination of decay rate.

The altitude of propagation was roughly estimated to be around 84km from the Earth's surface, indicated by the red arrow in Figure 5. This estimation almost has a good agreement with the referred altitude foreseen by spaceflight101 (https://spaceflight101.com/), which predicted the occurrence of re-entry over a specific region that denotes the 80km passage between latitudes 43° north and 43° south.

The coverage available for a particular region is evaluated through an instantaneous field of view or typically called a footprint, on which a particular area appears as the spacecraft

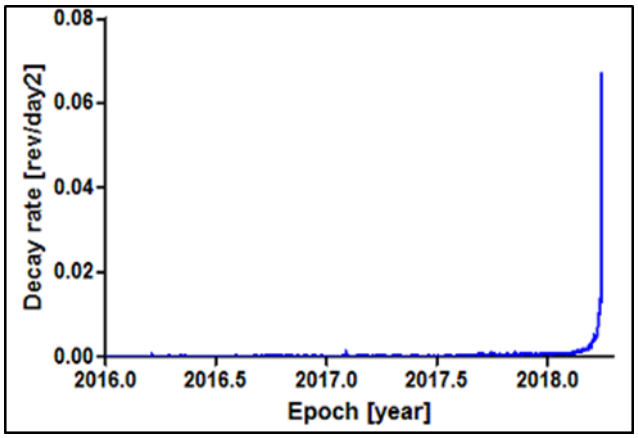

Figure 4. The approximate decay rate of Tiangong-1 from 2016 to 2018.

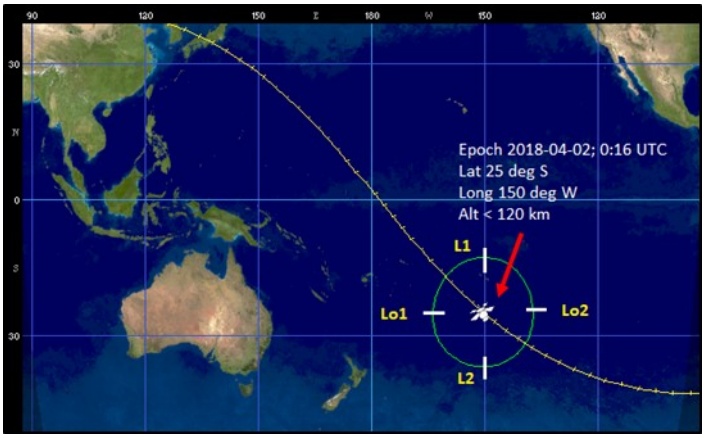

Figure 5. The re-entry point of Tiangong-1 on April 2, 2018 at 0:16 UTC

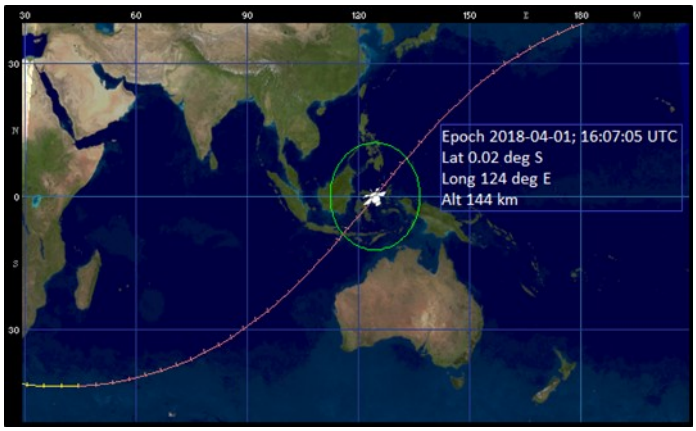

Figure 3. Tiangong-1 position based on the latest TLE set data on April 1 2018

Table 1. The disparted points of footprint concerning re-entry incident

Coordinate	Position 1	Position 2	Delta (Δ)
Longitude (Lo°/*l*°)	163.87 W	137.77 W	26.1
Latitude (L°/ *f*°)	12.82 S	37.07 S	24.25

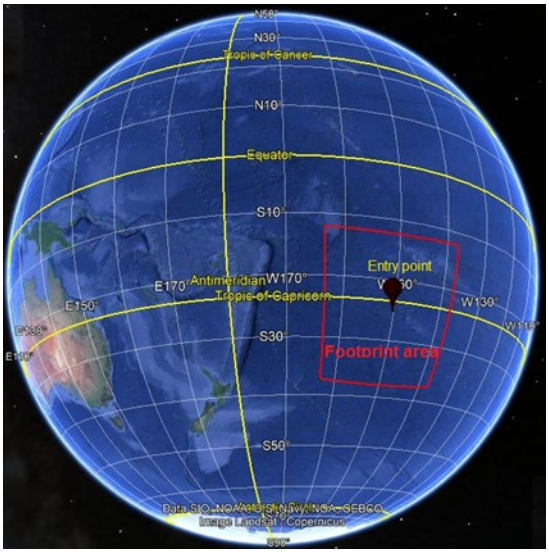

Figure 6. Location of footprint of Tiangong-1, indicated by the red square. The entry point lies on the center of the footprint area. Note that Google Earth has been used to overlay the footprint area.

moves along. This footprint is indicated by the green oval in Figure 5. Furthermore, an assumption was made that the debris will fall inside the footprint. Also, to assess the size of the footprint, each of the two major points of latitude (L1 and L2) and longitude (Lo1 and Lo2) are simply disparted as presented in Table 1.

The approximate latitude of Tiangong-1 during the re-entry incident was about 25° S. The dimension of footprint area on Earth is appraised by applying the following equations

$$\lambda\,(km) = \left(\frac{\Delta\lambda}{360°} x 2\pi x Re\right)\cos(\phi) \quad (1)$$

$$\phi\,(km) = \frac{\Delta\phi}{360} x\ 2\pi\ x\ Re \quad (2)$$

Here, *Re* designates equatorial radius of ~6378 km, and λ as well ϕ represent latitude and longitude blanketings, respectively. Imposing entire parameters in Table 1 into equations (1) and (2), the dimension of a footprint around 2,632 km x 2,698 km was derived as shown in Figure 6.

Figure 6 describes the estimated area of falling debris of Tiangong-1 broken down over the South Pacific Ocean around midnight. Due to difficulty in estimating the exact location of impact as a single point, the spacecraft was likely to drop somewhere inside the predicted area marked by the red square presented in Figure 6 with an uncertainty window around 21,832 km x 21,898 km. This is appraised based on some re-entry cases and decay analyses which are ±20% of a residual lifetime to accommodate uncontrolled re-entry prediction(Pardini & Anselmo, 2013). In this study, the uncertainty is corresponded to ±0.48 orbits. With regard to the complexity of an accurate prediction of the footprint area (Weaver et al., 2001), the difficulty arises from the uncertainty of drag dependence on ballistic coefficient and atmospheric density, which vary in time, leading to an erroneous model. Furthermore, a cross-track dispersion of debris trajectories emerges due to the local wind factor as it reaches the lower atmosphere (Falsone et al., 2014 and references therein). Notwithstanding, all perturbation factors described above were neglected in this study, however, complexity still existed indicated by a vast territory of falling debris.

Subsequently, the footprint area was calculated by adopting several equations in Astrodynamics with the notion that the Earth's curvature was negligible. To do this, the impact on the area served as the target (P), while the spacecraft remained at the re-entry point. The following equations were exploited:

$$L = S \sin\ \theta / \sin\ \varepsilon \quad (3)$$

$$W = S \sin\theta \quad (4)$$

L and W indicate the length and width of the footprint, respectively, S represents the distance of spacecraft to the target, θ and ε denote angular width of footprint, and the spacecraft elevation angle. The geometry of footprint (Larson & Wertz, 1999) is frugally illustrated in Figure 7.

By specifying the values of $S \approx 1038.5$ km, $\theta \approx 0.67°$ and $\varepsilon \approx 3.5°$, the approximate footprint is determined to be around 193km x 12km with an uncertainty window of approximately 19,393km x 19,212km, which is much smaller than the previous determination. Notice that the values of S, θ, and ε above were derived by considering the angular radius of the horizon around 9.3°, proportional to the distance between the spacecraft and the target (S).

A discrepancy exists between the footprint determination from propagated TLE data set (the first method) and calculation (the second method). However, they both disregard perturbation from the atmospheric drag and the local wind. The results remain distinct on account of several points as follows:

1. As previously mentioned that the second method disregarded the inclusion of the Earth's curvature in the second method, which influences the projection of the surface footprint In the inertial space spanning from 20.6° to 25.6° (Lin et al., 2019) and affected the determination.
2. The choice of target point coordinate in the second method is comparatively inadequate, leading to

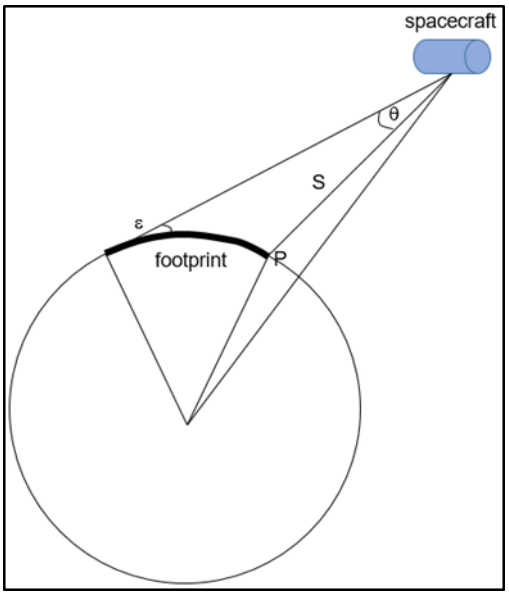

Figure 7. Illustration of footprint geometry with respect to the re-entry point (Adopted from Larson and Wertz, 1999 with a bit of adjustment)

Table 2. Comparison of approaches in case of Tiangong-1's re-entry

Approach	Present study		Choi et al. (2017)
	Method 1	Method 2	
Footprint length (km)	2,632	192	9,000
Method	Orbital propagation		DRAMA SARA

erroneous elevation angle of spacecraft. The problem is that the location of debris impact (target point) is not properly considered rather than lucrative supposition owing to dampen the footprint area.

3. The inaccuracy of spacecraft elevation angle is due to the entanglement of linear approximation in its formulation. The smaller the elevation angle gets close to the horizon, the greater the error of the footprint length. In addition, the propagation of the orbit also affects the accuracy of the determination.

Considering all the above points, it appears that the footprint determination from the first method is more tolerable than the second. Furthermore, the dimension of footprint, referring to the nominal re-entry point of 84km and apart from the exact calculation, is the order of thousands of kilometers proportional to the order of size gained from other studies (Klinkrad, 2006; Choi et al., 2017). Nevertheless, there is a need to re-emphasize that the assumption has been undertaken at which Tiangong-1 debris fell inside the footprint circle described in Figure 6, and it corresponded to the Southern Pacific Ocean.

In addition, the results from the two aforementioned methods were compared with other studies. In the case of Tiangong-1's re-entry, a quite similar study was found, as presented in Table 2.

Table 2 showed that the average dimension of footprint area is of the order of several thousand kilometers. It is important to point out that these results, including the accuracy depend on the method and the assumption used in the study. This is one reason why the accuracy in footprint determination is still problematic due to many factors involved.

4. Conclusion

The accurate determination of footprint area due to re-entry space debris is hard to predict because of the many factors involved. Propagation of the last TLE set and the Mathematical formulation in Astrodynamics was exploited to determine the footprint area of falling space debris using Tiangong-1 as a case study. To propagate the spacecraft trajectory using the last TLE data until the spacecraft hits the re-entry point, the decay rate and average loss were required. Some assumptions were used in which the effects of tropospheric wind, the rate of Earth's rotation, atmospheric density, the influence of solar, and geomagnetic activities were excluded for practical purposes. It was estimated that the spacecraft re-entered the atmosphere at around 84km altitude. Since its inclination was around 43°, the coverage area of falling debris stretched over 43° North and South latitudes. Furthermore, the footprint was determined by exerting each of the two major points of latitude and longitude at the altitude of the re-entry point altitude. In the absence of perturbation factors, the conjectured area of falling Tiangong-1 was of the order of thousands of kilometers (2,632km x 2,698km) as described in Figure 6.

Furthermore, a particular formulation in Astrodynamics was adopted to confirm the dimension of footprint area from the propagated TLE method as previously mentioned. This undertook a linear approximation, which resulted in a large error in the length of the footprint as the spacecraft gets closer to the horizon. Nevertheless, the dimension of the area is much smaller, with the length of ~1/13th of the footprint from the first method (193 km x 12 km). The exclusion of the Earth's curvature, including such speculation in determining the target point led to a large degree of uncertainty in the determination of footprint and became unreasonable. Therefore, the plausible dimension of footprint area for the falling debris of Tiangong-1 was appointed to the first method where the decommissioned spacecraft fell over the Southern Pacific Ocean. Conclusively, it is important to note that these study results are not totally precise and need further investigation to obtain high accuracy.

Abbreviations

SIA : Satellite Industry Association
ASAT : Anti Satellite
DEB : Debris
SSN : Space Surveillance Network
TLE : Two Line Element
NASA : National Aeronautics and Space Administration
LEO : Low Earth Orbit
SGP4 : Simplified General Perturbation 4
UTC : Coordinated Universal Time

Acknowledgement

The main author, as the main contributor of the present article, would like to thank LAPAN under Space Science Center to facilitate research and provide research funding. The main author would also like to thank Space-Track to provide access to spacecraft orbital data. Lastly, the authors would also like to thank reviewers and editors for their suggestions and effort to improve the quality of manuscript.

References

Choi, E. J., Cho, S., Lee, D. J., Kim, S., & Jo, J. H. (2017). A study on re-entry predictions of uncontrolled space objects for space situational awareness. *Journal of Astronomy and Space Sciences*, *34*(4), 289–302. https://doi.org/10.5140/JASS.2017.34.4.289

Csillik, I. S. (2017). Analysis and Prediction of Tiangong-1 Reentry Analysis and Prediction of Tiangong-1 Reentry. *Romanian Astron. J.*, *27*(3).

Falsone, A., Noce, F., & Prandini, M. (2014). A randomized approach to space debris footprint characterization. *IFAC Proceedings Volumes*, *47*(3), 6895–6900. https://doi.org/10.3182/20140824-6-ZA-1003.00612

Kelso, T. S., Parkhomenko, N. N., Shargorodsky, V. D., Vasiliev, V. P., Yurasov, V. S., Nazarenko, A. I., Tanygin, S., & Hiles, R. M. (2013). What Happened to BLITS? An Analysis of the 2013 Jan 22 Event. *The 14th Annual Advanced Maui Optical and Space Surveillance Conference (AMOS), September.* http://www.amostech.com/TechnicalPapers/2013/Orbital_Debris/KELSO.pdf

Kennewel, J. (1999). Satellite Orbital Decay Calculations. In *IPS*

Radio and space Service. http://www.ips.gov.au/Category/Educational/Space Weather/Space Weather Effects/SatelliteOrbitalDecayCalculations.pdf

Klinkrad, H. (2006). Space Debris Models and Risk Analysis. In *Springer-Verlag Berlin Heidelberg New York*. Praxis Publishing.

Larson, W. J., & Wertz, J. R. (1999). *Spacecraft Mission Analysis and Design*. California and Kluwer Academic Publishers. https://the-eye.eu/public/WorldTracker.org/Space/Space Engineering/Space_Mission_Analysis_and_Design.pdf

Lin, H. Y., Zhu, T. L., Liang, Z. P., Zhao, C. Y., Wei, D., Zhang, W., Han, X. W., Zhang, H. F., Wei, Z. Bin, Li, Y. Q., Xiong, J. N., Zhan, J. W., Zhang, C., Ping, Y. D., Song, Q. L., Zhang, H. T., & Deng, H. R. (2019). Tiangong-1's accelerated self-spin before reentry. *Earth, Planets and Space*, *71*(1). https://doi.org/10.1186/s40623-019-0996-8

NASA. (2014). Orbital debris. In *Orbital Debris Quarterly News* (Vol. 18, Issue 1, pp. 1–10). https://orbitaldebris.jsc.nasa.gov/quarterly-news/pdfs/odqnv18i1.pdf

Pardini, C., & Anselmo, L. (2013). Reentry predictions of three massive uncontrolled spacecraft. *The 6th IAASS Conference – Safety Is Not an Option*, *May*.

SIA. (2017). *State of the Satellite Industry Report* (Issue June). https://www.nasa.gov/sites/default/files/atoms/files/sia_ssir_2017.pdf

Stamminger, A. (2007). Atmospheric re-entry analysis of sounding rocket payloads. *The 18th ESA Symposium on European Rocket and Balloon Programmes and Related Research, June*, 1–15.

Stansbery, E. G. (2004). Growth in the number of SSN tracked orbital objects. *The 55th International Astronautical Congress of the International Astronautical Federation, the International Academy of Astronautics, and the International Institute of Space Law*, 1–5. https://doi.org/10.2514/6.iac-04-iaa.5.12.1.03

Tan, A., Zhang, T. X., & Dokhanian, M. (2013). Analysis of the Iridium 33 and Cosmos 2251 Collision Using Velocity Perturbations of the Fragments. *Advances in Aerospace Science and Applications*, *3*(1), 13–25.

Vallado, D. A. (2001). *Fundamentals of astrodynamics and applications*. McGraw-Hill.

Vallado, D. A., Crawford, P., Hujsak, R., & Kelso, T. S. (2006). Revisiting spacetrack report #3. *AIAA/AAS Astrodynamics Specialist Conference and Exhibit, August*. https://doi.org/10.2514/6.2006-6753

Vellutini, E., Bianchi, G., Perozzi, E., Pardini, C., Anselmo, L., Pisanu, T., Di Lizia, P., Piergentili, F., Monaci, F., Reali, M., Villadei, W., Buzzoni, A., Amore, G. ., & Muolo, L. (2020). Monitoring the final orbital decay and the re-entry of Tiangong-1 with the Italian SST ground sensor network. *Journal of Space Safety Engineering*, *7*(4), 487–501. https://doi.org/10.1016/j.jsse.2020.05.004

Weaver, M. A., Baker, R. L., & Frank, M. V. (2001). Probabilistic estimation of reentry debris area. *The 3rd European Conference on Space Debris, ESOC, March*.